

# Subtype-Specific Synaptic Proteome Alterations in Sporadic Creutzfeldt-Jakob Disease

Joanna Gawinecka<sup>a,1</sup>, Martin Nowak<sup>a,1</sup>, Julie Carimalo<sup>a</sup>, Franco Cardone<sup>d</sup>, Abdul R. Asif<sup>b</sup>, Wiebke M. Wemheuer<sup>c</sup>, Walter J. Schulz-Schaeffer<sup>c</sup>, Maurizio Pocchiari<sup>d</sup> and Inga Zerr<sup>a,\*</sup>

<sup>a</sup>National Reference Center for TSE, Medical Center Georg-August University, Goettingen, Germany

<sup>b</sup>Department of Clinical Chemistry, Medical Center Georg-August University, Goettingen, Germany

<sup>c</sup>Department of Neuropathology, Medical Center Georg-August University, Goettingen, Germany

<sup>d</sup>Department of Cell Biology and Neurosciences, Istituto Superiore di Sanità, Rome, Italy

Handling Associate Editor: Ottavio Arancio

Accepted 25 April 2013

**Abstract.** Sporadic Creutzfeldt-Jakob disease (sCJD) is characterized by wide clinical and pathological variability, which is mainly influenced by the conformation of the misfolded prion protein (PrP<sup>Sc</sup>) and by methionine and valine polymorphism at codon 129 of the gene encoding PrP. This heterogeneity likely implies differences in the molecular cascades that lead to the development of certain disease phenotypes. Here, we investigated synaptic proteome patterns in two most common sCJD subtypes (MM1 and VV2) using 2D DIGE and mass spectrometry. We found that 23 distinct proteins were differentially expressed in at least one sCJD subtype when compared to age-matched controls. The majority of these proteins displayed significant subtype-specific alterations, with only up-regulated glial fibrillary acidic protein and down-regulated spectrin alpha chain in both sCJD subtypes. Differentially expressed proteins found in this study are mainly involved in synaptic structure and activity, mitochondrial function, or calcium metabolism. Moreover, several of them have been already linked to the pathophysiological processes occurring in Alzheimer's disease.

**Keywords:** Creutzfeldt-Jakob disease, 2D fluorescence difference gel electrophoresis (2D DIGE), proteomics, sCJD, synapse, synaptic dysfunction

## INTRODUCTION

Sporadic Creutzfeldt-Jakob disease (sCJD), the most common form of human transmissible spongiform encephalopathy, displays a broad heterogeneity of clinical and pathological features. Disease phenotype is mainly influenced by the methionine/valine

(M/V) polymorphism at codon 129 in the human prion protein gene (*PRNP* gene) and by the presence of two major types of pathological, protease-resistant forms of prion protein (PrP<sup>Sc</sup>) leading to two different profiles in Western blot (type 1 and type 2), giving six possible combinations: MM1, MM2, MV1, MV2, VV1, and VV2 [1]. The major subtypes of sCJD are homozygotes for methionine at codon 129 in *PRNP* gene with PrP<sup>Sc</sup> type 1 (MM1) and homozygotes for valine at codon 129 in *PRNP* gene with PrP<sup>Sc</sup> type 2 (VV2), representing about 67% and 15% of all sCJD cases, respectively. The clinical and pathological characteristics of the molecular disease subtypes differ markedly with respect to symptoms at onset, localization and

<sup>1</sup>These authors contributed equally to the work.

\*Correspondence to: Inga Zerr, Prion Research Group, National Reference Center for TSE, Department of Neurology, University Medical School, Georg-August University, Robert-Koch Street. 40, 37075 Göttingen, Germany. Tel.: +49 (0)551/39 6636; Fax: +49 (0)551/39 7020; E-mail: epicjd@med.uni-goettingen.de.

type of the pathological changes as well as PrP<sup>Sc</sup> deposition pattern [1, 2]. For instance, MM1 subtype is a myoclonic type with cognitive impairments accompanied by mental and visual signs at the disease onset while VV2 is an ataxic type, where dementia is developed later in disease progression. Differences between subtypes can be also found in the brain histopathology. The topography of MM1-associated lesions shows that the rostral regions are more severely affected than the caudal ones, while in the VV2, it is the opposite [2]. Such a high degree of heterogeneity might suggest involvement of different molecular partners and/or pathways in sCJD pathogenesis depending on the PrP misfolded form.

Beside the spongiform changes or severe gliosis, neuronal loss and dysfunction are a fundamental and constant feature of animal and human prion diseases [3, 4]. Interestingly, synaptic loss and degeneration of the axon terminal preceded neuronal loss in the hippocampus of ME7-infected mice, and it occurs even before clinical manifestation of the disease [5]. Electron microscope study showed the presence of abnormally shaped synapses in which the postsynaptic membrane modifies its curvature in the intrahippocampally injected ME7 prion model [6]. Moreover, Western blot analysis showed PrP<sup>Sc</sup> accumulation in the synaptosomal fractions isolated from scrapie infected hamsters [7].

Therefore, determining proteins involved in pathophysiological processes responsible for synaptic failure may increase our knowledge of molecular mechanisms underlying onset of clinical signs and open new ways for the diagnosis and treatment of human prion diseases.

In this study, we analyzed prion-induced synaptic proteome alterations in the two most frequent subtypes of sCJD: MM1 and VV2. Our data revealed that 23 distinct proteins showed altered expression levels due to the PrP<sup>Sc</sup> presence in the brain tissue. Interestingly, only one isoform of the glial fibrillary acidic protein (GFAP) displayed a significant up-regulation in both analyzed subtypes. Furthermore, two isoforms of spectrin alpha chain were down-regulated (isoform with ID 6355 was specific for MM1 while isoform with ID 10783 was specific for VV2). Remaining proteins were differentially expressed either in the MM1 or VV2 subtype. Differentially expressed proteins found in this study are mainly involved in synaptic structure and activity, mitochondrial function, or calcium metabolism. Moreover, several of them have been linked to the pathophysiological processes occurring in Alzheimer's disease (AD).

## PATIENTS, MATERIALS, AND METHODS

### *Patients*

Samples from the frontal cortex were obtained from 10 pathologically confirmed sCJD patients (5 with MM1 and 5 with VV2 subtype) and 5 age-matched control cases (CON). The mean age for the MM1, VV2, and CON group was  $71 \pm 7$ ,  $68 \pm 6$ , and  $69 \pm 7$  years, respectively. Histopathological examination of the brain tissues revealed spongiform changes and prion protein (PrP<sup>Sc</sup>) depositions in all sCJD patients while only insignificant age-related changes of the brain structure and neuronal morphology were observed in control cases (no signs of intracranial pressure, bleeding, or vascular changes). Control patients were diagnosed with multi-organ dysfunction syndrome, chronic kidney dysfunction, lung cancer, or myocardial infarction. The sCJD patients showed typical disease duration as well as clinical and neuropathological findings. The mean disease duration of MM1 and VV2 subtype was  $4 \pm 2$  and  $8 \pm 2$  months, respectively. Moreover, all sCJD patients were demented and positive for 14-3-3 protein in CSF. Three MM1 and four VV2 patients displayed hyperintensity in the basal ganglia detected by T2-weighted MRI while the presence of periodic sharp wave complexes (PSWC) in EEG was detected in one MM1 and all VV2 patients. Moreover, pattern of PrP-depositions in MM1 cases was punctuate while some perineuronal and plaque-like aggregates were detected in VV2 cases.

The postmortem delay was around 24 h for all analyzed samples. Until autopsy procedure, corpses were stored at 4°C.

### *2D fluorescence difference gel electrophoresis (2D-DIGE)*

#### *Synaptosome preparation*

Samples from the frontal cortex were stored at  $-80^{\circ}\text{C}$  prior to analysis, and synaptosomal fractions were prepared at the same time. Tissue samples were homogenized in 5 volumes of homogenization buffer (H buffer) containing 20 mM HEPES (pH 7.4), 0.32 M sucrose, 1 mM sodium orthovanadate, 1 mM EDTA and Complete Protease Inhibitor Cocktail (Roche), using a glas-teflon homogenizer. Brain homogenates were centrifuged at  $1,500 \times g$  for 10 min to remove unhomogenized tissue parts. Supernatants were retained and centrifuged again at  $15,000 \times g$  for 10 min. The pellets were resuspended in 1 ml of H buffer and layered over discontinuous sucrose gradient

(0.85 M pH 7.4, 1 M pH 7.4, 1.2 M pH 8.5 sucrose solutions, supplemented with 10 mM HEPES and 2 mM EDTA) and spun at  $82,500\times g$  for 1 h at  $4^{\circ}\text{C}$ . Synaptosomes were collected from 1 M and 1.2 M sucrose interface, washed with 5 volumes of H buffer and centrifuged at  $20,000\times g$  for 20 min at  $4^{\circ}\text{C}$ . Finally, pellets containing synaptosomal fraction were resuspended in 0.5 ml H buffer and stored at  $-80^{\circ}\text{C}$  and at  $-20^{\circ}\text{C}$ .

#### 2D-DIGE and 2D image analysis

Prior to analysis, protein concentration was determined using Bradford Protein Assay (Bio-Rad). 25  $\mu\text{g}$  of protein were precipitated overnight with acetone-methanol (8:1; vol:vol) at  $-20^{\circ}\text{C}$  and centrifuged at  $16,000\times g$  for 15 min. The pellet was resuspended in 10  $\mu\text{l}$  of lysis buffer containing 7 M urea, 2.5 M thiourea, 4% CHAPS, 30 mM TRIS, and 5 mM magnesium acetate and subsequently labeled with 100 pmol of CyDye (GE Healthcare) as follows: pooled samples as internal standard with Cy2, individual control, and sCJD samples with either Cy3 or Cy5. The dye-switch between control and sCJD samples was done in order to avoid dye-to-protein preferences.

Labeling reaction was performed on ice in the dark for 30 min, terminated by adding 10 mM lysine and incubation for an additional 10 min. Equal volume of a lysis buffer containing 130 mM DTT and 0.8% 3–10 Bio-Lyte (Bio-Rad) was added to the labeling mixture. Then samples were mixed together, diluted up to 350  $\mu\text{l}$  with a rehydration buffer composed of 7 M urea, 2.5 M thiourea, 4% CHAPS, 0.2% 3–10 Bio-Lyte, and 65 mM DTT and loaded on ReadyStrip IPG non-linear pH 3–10, 17 cm strip (Bio-Rad). After 12 h of active rehydration at 50 V, isoelectric focusing was initiated at 500 V for 1 h, followed by ramping at 1,000 V for 1 h and 5,000 V for 2 h. The final focusing was carried out at 8,000 V reaching a total of 60,000 Vh using PROTEAN IEF CELL (Bio-Rad). The strips were then equilibrated twice for 20 min in a buffer containing 6 M urea, 2% SDS, 30% glycerin, and 150 mM Tris, pH 8.8, supplemented with 2% DTT in the first, and with 2.5% iodoacetamide in the second equilibration step. SDS-PAGE was performed overnight with homogenous 12% polyacrylamide gel and constant 20 mA using Protean II XL Cell (Bio-Rad). CyDye-labeled protein gels were scanned by three different lasers with band pass filtered emission wavelengths of 510 nm (Cy2), 575 nm (Cy3), and 665 nm (Cy5) using FLA-5100 imaging system (Fujifilm).

Protein spot abundances within 20 brain proteome patterns (5 MM1, 5 VV2, 5 CON, and 5 internal samples) were analyzed using the Delta2D software (v. 3.6)

(DECODON). Differences in spot abundance detected by densitometric analysis were statistically evaluated using the unpaired Student's *t*-test. A protein spot was considered differentially expressed when its densitometric analyses showed at least 2-fold change in abundance was accompanied by a *p*-value  $<0.05$  in the unpaired Student's *t*-test.

#### Preparative 2D gels and protein identification

To identify differentially expressed protein spots, the preparative 2D gels containing 350  $\mu\text{g}$  protein were prepared as described above (DIGE-staining procedure was omitted). To reduce the infectivity of synaptic extracts and to minimize the risk of infection for laboratory staff, samples were boiled at  $95^{\circ}\text{C}$  in 5% SDS for 10 min [8–11] before precipitation with acetone-methanol (8:1; vol:vol) at  $-20^{\circ}\text{C}$ . After gel electrophoresis was terminated, gels were stained with colloidal Coomassie staining solution according to the protocol given by Candiano et al. [12]. Gel plugs containing visualized proteins of interest were manually excised from gels and subjected to in-gel digestion. The detailed protocol of this procedure is given by Ramljak et al. [13]. In-gel digested peptides were dissolved in 0.1% TFA followed by injection into the Q-TOF Ultima Global mass spectrometer (Micromass, Manchester, UK) as previously described [14]. The data were acquired with the MassLynx (v 4.0) software on a Windows NT PC and further processed using ProteinLynx Global Server (PLGS, v 2.2, Micromass, Manchester, U.K.) as PKL (peak list) under the following settings: electrospray, centroid 80% with minimum peak width 4 channel, noise reduction 10%, Savitzky-Golay, MSMS, medium deisotoping with 3% threshold, no noise reduction, and no smoothing. The peaklists were searched out using the online MASCOT algorithm against the SwissProt 2011\_07 (530264 sequences; 1879410742 residues). The data obtained were retrieved against the whole database with search parameters set as follows: enzyme, trypsin; allowance of up to one missed cleavage peptide; mass tolerance  $\pm 0.5$  Da and MS/MS tolerance  $\pm 0.5$  Da; modifications of cysteine carboamidomethylation and methionine oxidation when appropriate with auto hits allowed only significant hits to be reported.

#### Western blotting

25  $\mu\text{g}$  of proteins were separated on 12% SDS-PAGE gel and transferred to PVDF membrane. Membrane was blocked with 5% skimmed milk in phosphate buffer saline with 0.2% Triton X-100 (TBST) for 1 h at room temperature. Subsequently,

membranes were incubated overnight at 4°C with one of the following primary antibodies: mouse anti-annexin A6 (1:1000, ECMBiosciences), mouse anti-spectrin alpha chain (1:2000, Abcam), mouse anti- $\beta$ -actin (1:7500, Abcam), rabbit anti-syntaxin-binding protein 1 (1:500, LifeSpan BioSciences), or rabbit anti-synaptophysin (1:2000, Dako Cytomation). Thereafter, membranes were washed with PBST and incubated for 1 h at room temperature with a corresponding horseradish peroxidase-conjugated secondary antibody: goat anti-rabbit (1:5000, Jackson Research) or goat anti-mouse (1:5000, Jackson Research). The immunoreactivity was detected after immersion of the membranes into enhanced chemiluminescence (ECL) solution and exposition to ECL-Hyperfilm (Amersham Biosciences). The film was scanned and densitometric and statistical analysis was performed with ImageJ (Image Processing and Data Analysis free software) and Sigmaplot (Exact Graphs and Data Analysis software, Systat), respectively. The protein was considered as specific sCJD-regulated when a  $p$ -value was lower than 0.05 in Kruskal-Wallis ANOVA with Tukey's range test.

## RESULTS

### *Synaptosome isolation*

A proper and efficient isolation of synaptosomes was proven by Western blot analysis directed against synaptophysin, which is a major protein component of a synaptic vesicle membrane (Fig. 1). Positive immunostaining was detected only in the synaptic fraction confirming proper isolation of the fraction of interest.

### *Comparative brain proteome analysis using 2D-DIGE*

Using 2D-DIGE technology and Delta2D's 100% spot matching approach, around 260 protein spots could be detected on synaptic proteome patterns.

Densitometric and statistical analysis revealed 40 protein spots (15% of all detected protein spots) with significantly altered expression level in at least one sCJD subtype when compared to age-matched controls. Proteins were identified from 29 out of 40 protein spots. From remaining 11 protein spots identification was not possible due to not detectable or very faint staining on colloidal Coomassie stained preparative gel (Fig. 2 and Table 1).

The expression level of sCJD-related proteins did not show any significant differences between MM, MV,

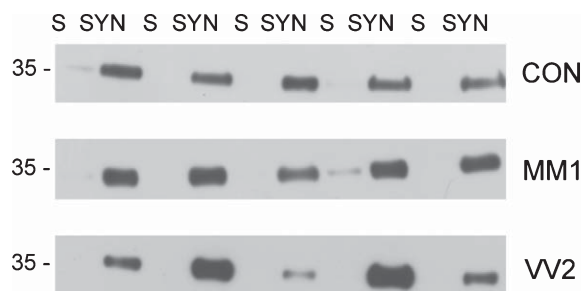


Fig. 1. Western blot analysis of synaptosomes isolation. After centrifugation steps, supernatants (S) containing soluble proteins were discarded and pellets were utilized to isolate synaptosomes (SYN) by the ultracentrifugation in the sucrose gradient. The Western blot obtained after immunodetection using specific antibody raised against synaptophysin, a synaptic specific marker, confirmed the isolation of synaptic fraction from the brain homogenates.

and VV genotypes in the control group, except for 14-3-3 protein epsilon and gamma isoform. It appears that valine at codon 129 is associated with a lower 14-3-3 level while methionine with a higher 14-3-3 level (data not shown).

Identified protein spots correspond to 23 distinct proteins. In both analyzed subtypes, significant up-regulation was observed for one isoform of the glial fibrillary acidic protein (GFAP, ID 6805) and down-regulation was observed for two isoforms of spectrin alpha chain (isoform with ID 6355 was specific for MM1 while isoform with ID 10783 was specific for VV2 subtype). However, the  $p$ -value at 0.053 for protein spot with ID 6355 lies just above significance level, and it is likely that under other experimental conditions, it would reach statistical significance level. Remaining proteins showed subtype-specific differential expression.

Overall, differentially expressed proteins found in this study were clustered into four distinct groups according to their biological function: proteins belonging to cell structure and transport, proteins of the cellular metabolism, proteins related to apoptosis and oxidative stress, and proteins involved in protein folding (Fig. 3 and Table 1).

### *Differentially expressed proteins in sCJD versus control*

#### *Proteins belonging to cell structure and transport*

This group includes above mentioned GFAP isoform, spectrin alpha chain, and several proteins specific for certain subtype. Around 3-fold up-regulated gel-solin isoforms, GFAP (ID 6810 and 6811) as well

Table 1  
 List of differentially expressed proteins in synaptosomal fractions isolated from the frontal cortex. A protein spot was considered to be differentially expressed when its densitometric analyses showed at least a 2-fold change in abundance (MM1 and VV2 subtypes versus control or MM1 versus VV2), which was accompanied by a *p*-value <0.05 in unpaired Student's *t*-test. Differentially expressed proteins were clustered into four distinct groups according to their biological functions (cell structure and transport, apoptosis and oxidative stress, and protein folding). CON indicates differential expression in both analyzed subtypes versus control, and MM1 and VV2 indicate differential expression specific for the MM1 or VV2 subtypes versus control, respectively. In bold are marked proteins that show significant differential expression between two analyzed subtypes

ID	Protein name	MM1 subtype versus control		VV2 subtype versus control		MM1 versus VV2 subtype		UniProt access.	MW (kDa)	pI	Score	Queries matched
		fold of change	<i>p</i> -value	fold of change	<i>p</i> -value	fold of change	<i>p</i> -value					
<b>Cell structure and transport</b>												
6805	Glial fibrillary acidic protein (GFAP) <sup>CON</sup>	2.00	0.010	2.35	0.010	0.98	0.952	P14136	50	5.4	398	8
6810	GFAP <sup>MM1</sup>	2.76	0.029	2.01	0.059	1.37	0.546	P14136	50	5.4	177	4
6811	GFAP <sup>MM1</sup>	3.18	0.004	2.30	0.103	1.38	0.504	P14136	50	5.4	302	6
6488	Gelsolin <sup>MM1</sup>	3.03	0.014	2.20	0.159	1.38	0.562	P06396	85.6	5.9	143	4
6491	Gelsolin <sup>MM1</sup>	2.57	0.026	2.13	0.207	1.21	0.761	P06396	85.6	5.9	178	4
<b>6986</b>	<b>Tubulin beta chain</b> <sup>VV2</sup>	<b>0.94</b>	<b>0.903</b>	<b>2.43</b>	<b>0.040</b>	<b>0.39</b>	<b>0.042</b>	<b>Q13885</b>	<b>50</b>	<b>4.8</b>	<b>174</b>	<b>3</b>
6355	Spectrin alpha chain, brain <sup>MM1</sup>	0.28	0.043	0.31	0.053	0.90	0.853	Q13813	284	5.2	60	5
10783	Spectrin alpha chain, brain <sup>VV2</sup>	0.78	0.492	0.43	0.028	1.81	0.319	Q13813	284	5.2	164	6
6625	Syntaxin-binding protein1 <sup>MM1</sup>	0.49	0.029	0.65	0.089	0.75	0.333	P61764	67.5	6.5	154	10
9528	Annexin-A6 <sup>VV2</sup>	0.65	0.120	0.42	0.020	1.53	0.106	P08133	76	5.4	353	13
<b>7569</b>	<b>Ferritin heavy chain</b> <sup>MM1</sup>	<b>0.36</b>	<b>0.044</b>	<b>1.02</b>	<b>0.937</b>	<b>0.35</b>	<b>8.7E-04</b>	<b>P02794</b>	<b>21</b>	<b>5.3</b>	<b>95</b>	<b>4</b>
6532	Vesicle-fusing ATPase <sup>VV2</sup>	0.94	0.890	0.41	0.004	2.29	0.201	P46459	82.5	6.5	120	6
<b>Cellular metabolism</b>												
6499	Mitofilin <sup>VV2</sup>	3.24	0.090	2.63	0.028	1.23	0.741	Q16891	83.6	6.1	153	7
6543	NADH-ubiquinone oxidoreductase 75 kDa subunit <sup>MM1</sup>	2.71	0.042	0.99	0.937	2.75	0.121	P28331	79.4	5.9	291	5
6777	ATP synthase subunit alpha, mitochondrial <sup>MM1</sup>	0.33	0.013	0.65	0.179	0.49	0.100	P25705	59.7	9.2	793	10
<b>7387</b>	<b>Enoyl-CoA hydratase, mitochondrial</b> <sup>MM1</sup>	<b>0.31</b>	<b>0.010</b>	<b>1.23</b>	<b>0.492</b>	<b>0.25</b>	<b>0.028</b>	<b>P30084</b>	<b>31</b>	<b>8.3</b>	<b>120</b>	<b>2</b>
<b>7065</b>	<b>Malate dehydrogenase, mitochondrial</b> <sup>MM1</sup>	<b>0.43</b>	<b>0.040</b>	<b>0.89</b>	<b>0.680</b>	<b>0.48</b>	<b>0.036</b>	<b>P40926</b>	<b>35.5</b>	<b>8.9</b>	<b>326</b>	<b>7</b>
7081	Malate dehydrogenase, mitochondrial <sup>MM1</sup>	0.35	0.046	0.94	0.877	0.36	0.080	P40926	35.5	8.9	313	7
6929	Aspartate aminotransferase, mitochondrial <sup>MM1</sup>	0.42	0.002	0.75	0.157	0.56	0.035	P00505	47.5	9.1	665	10
6923	Fructose-bisphosphate aldolase A <sup>MM1*</sup>	0.40	0.011	0.78	0.332	0.51	0.037	P04075	39.4	8.3	5	5
<b>Apoptosis and oxidative stress</b>												
<b>7301</b>	<b>14-3-3 protein epsilon</b> <sup>MM1</sup>	<b>3.65</b>	<b>0.003</b>	<b>1.05</b>	<b>0.915</b>	<b>3.48</b>	<b>0.008</b>	<b>P62258</b>	<b>29</b>	<b>4.6</b>	<b>215</b>	<b>8</b>
<b>7339</b>	<b>14-3-3 protein gamma</b> <sup>MM1</sup>	<b>3.44</b>	<b>0.007</b>	<b>0.73</b>	<b>0.442</b>	<b>4.73</b>	<b>0.008</b>	<b>P61981</b>	<b>29</b>	<b>4.8</b>	<b>211</b>	<b>4</b>
7553	Peroxiredoxin-2 <sup>MM1</sup>	0.26	0.040	0.85	0.692	0.30	0.13	P32119	22	5.7	471	7
<b>7566</b>	<b>Phosphatidylethanolamine-binding protein 1 (PEBP1)</b> <sup>MM1</sup>	<b>0.34</b>	<b>0.008</b>	<b>1.05</b>	<b>0.854</b>	<b>0.32</b>	<b>0.023</b>	<b>P30086</b>	<b>21</b>	<b>7.0</b>	<b>301</b>	<b>5</b>
7025	N(G), N(G) dimethylargininedimethylamino hydrolase 1 (DDAH1) <sup>VV2*</sup>	0.94	0.681	0.48	0.003	1.95	0.01	O94760	31	5.3	314	7
<b>Protein folding</b>												
40267	Heat shock protein HSP 90 <sup>MM1</sup>	2.07	0.024	1.92	0.152	1.08	0.846	P07900	83	5	82	5
6542	78 kDa glucose-regulated protein (Grp78) <sup>MM1</sup>	2.82	0.012	1.65	0.132	1.71	0.093	P11021	72.3	5.1	75	3
<b>7216</b>	<b>Alpha crystallin B chain</b> <sup>MM1</sup>	<b>0.24</b>	<b>0.016</b>	<b>1.20</b>	<b>0.638</b>	<b>0.20</b>	<b>0.037</b>	<b>P02511</b>	<b>20</b>	<b>6.8</b>	<b>88</b>	<b>1</b>
<b>7593</b>	<b>Alpha-crystallin B chain</b> <sup>MM1</sup>	<b>0.21</b>	<b>0.003</b>	<b>1.25</b>	<b>0.596</b>	<b>0.16</b>	<b>8.1E-06</b>	<b>P02511</b>	<b>20</b>	<b>6.8</b>	<b>374</b>	<b>7</b>

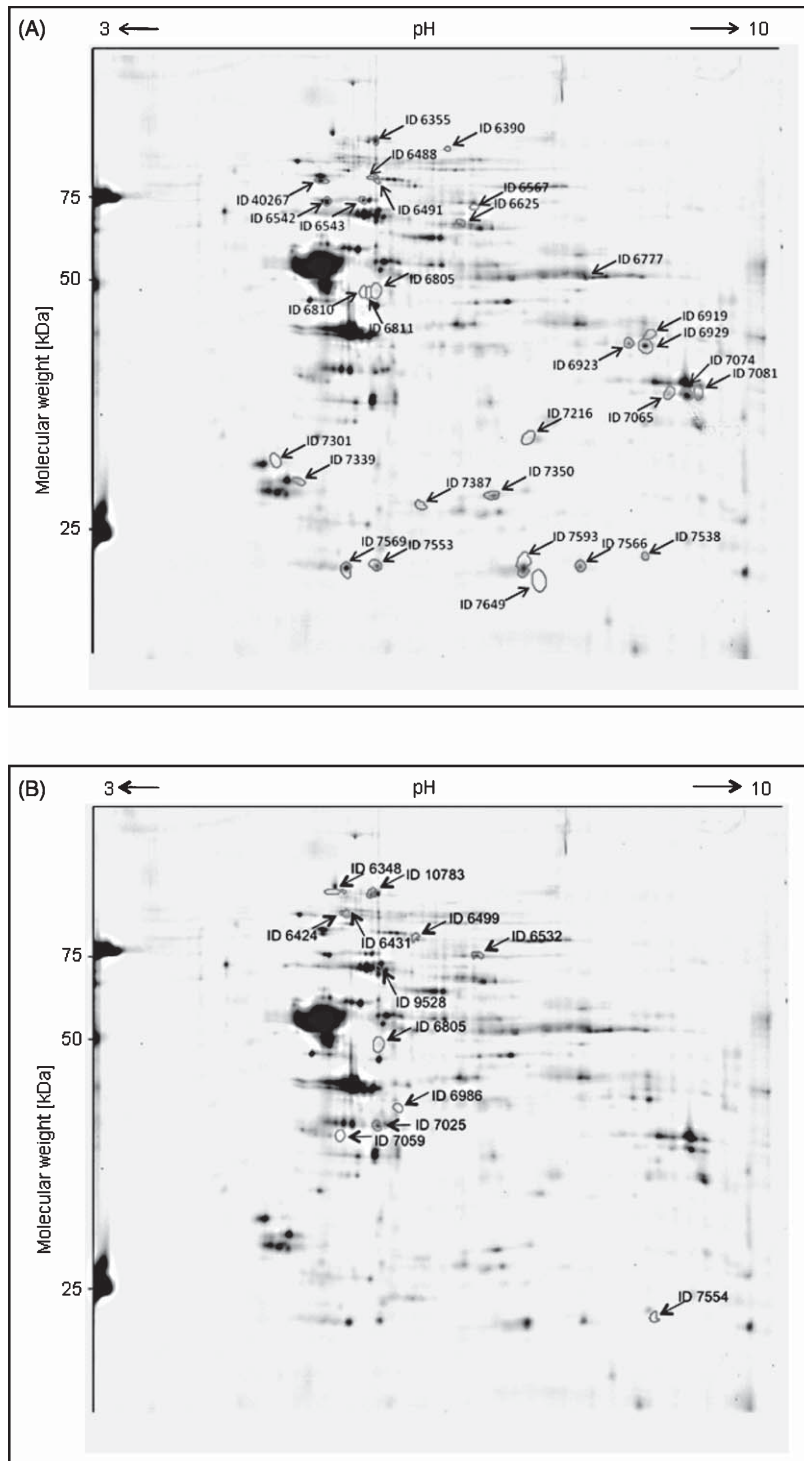


Fig. 2. 2D-maps of synaptosomal proteome. Differentially expressed proteins in the MM1 (panel A) and VV2 (panel B) subtypes versus age-matched controls are marked.

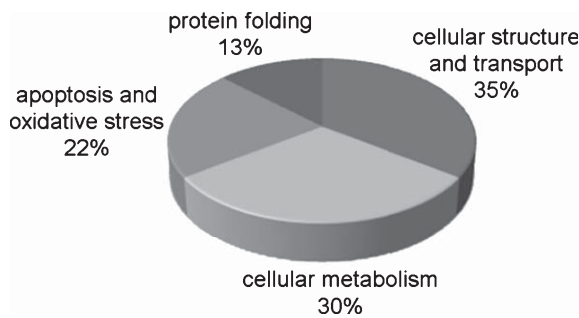


Fig. 3. Biological function of differentially expressed synaptic proteins. The differentially expressed proteins were categorized in four groups according to their biological function: cell structure and transport; cellular metabolism; apoptosis and oxidative stress; and protein folding (chaperon proteins). The pie chart indicates the impact of a single function alteration on the total classified functions.

as 2-3-fold down-regulated syntaxin-binding protein 1 and ferritin heavy, were specific for MM1 subtype. In turn, 2.4-fold up-regulated tubulin beta chain as well as 2.4-fold down-regulated annexin A6 and vesicle-fusing ATPase were specific for VV2 subtype.

#### *Proteins of the cellular metabolism*

Both core mitochondrial proteins mitofilin (VV2-specific) and NADH-ubiquinone oxidoreductase 75 kDa subunit were around 2.6-fold up-regulated while another mitochondrial protein called ATP synthase subunit alpha was 3-fold down-regulated. Two last mentioned proteins were specific for MM1 subtype. Moreover, all proteins implied in the lipid or energy metabolism (Enoyl-CoA hydratase, malate dehydrogenase, aspartate aminotransferase and fructose-bisphosphate aldolase A) displayed between 2.4 and 3.3-fold lower expression level solely in MM1 subtype.

#### *Proteins related to apoptosis and oxidative stress*

In the MM1 subtype, both 14-3-3 protein gamma and epsilon were 3.5-fold up-regulated while peroxiredoxin-2 and PEBP 1 were 3.8-fold and 2.9-fold down-regulated, respectively. In contrast, sole DDAH 1 protein was 2.1-fold down-regulated in VV2 subtype.

#### *Proteins involved in protein folding (chaperone proteins)*

Two proteins assisting in protein folding, namely heat shock protein 90 (Hsp90) and 78 kDa glucose-regulated protein (Grp78), displayed more than a 2-fold increased level, and alpha-crystallin B chain

showed more than a 4-fold decreased level in MM1 subtype. No VV2-specific protein was found in this functional group.

#### *Differentially expressed protein between sCJD subtypes*

Several proteins showed significant differential expression between the two analyzed sCJD subtypes. Tubulin beta chain, ferritin heavy chain, mitochondrial enoyl-CoA hydratase, mitochondrial malate dehydrogenase, PEBP1, and both alpha crystallin B chain isoforms were 0.16 to 0.48-fold down-regulated in the VV2 versus the MM1 subtype, while 14-3-3 protein was more than 3.5-fold up-regulated in the VV2 versus the MM1 subtype. For fructose-bisphosphate aldolase A and DDAH1, statistical requirement for a protein to be classified as differentially expressed was fulfilled; however, 1.95-fold of change in abundance was just below the 2-fold threshold.

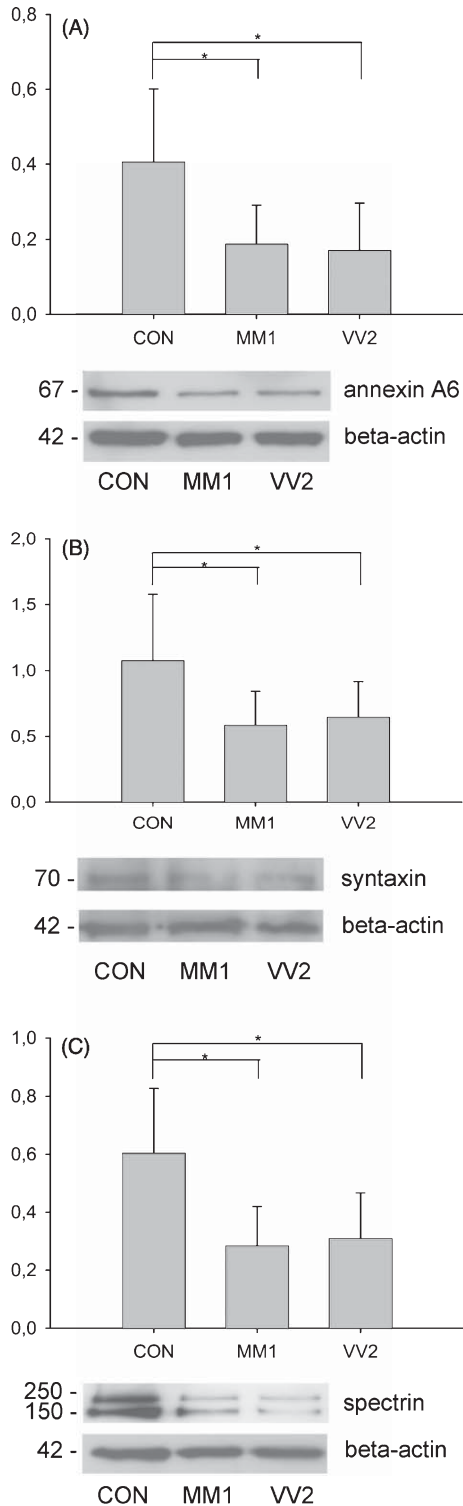
#### *Western blot analysis*

We focused our interest on three particular proteins (annexin A6, syntaxin-binding protein 1, and spectrin) likely linked to the synaptic dysfunction. The expression levels of these proteins were further analyzed by Western blotting in synaptosomal fractions from at least three different patients. All of them were significantly down-regulated in both sCJD subtypes in Western blot analysis though their decreased levels were significant in only one of sCJD subtypes in 2D-DIGE analysis (Fig. 4).

Annexin A6 immunoreactivity was 0.4-fold and 0.5-fold down-regulated in the MM1 and VV2 subtypes, respectively (Fig. 4A). Syntaxin-binding protein 1 was 0.6-fold down-regulated in both subtypes (Fig. 4B). Finally, spectrin level was 0.2-fold decreased in MM1 and 0.3-fold in VV2 subtype (Fig. 4C). For all computed statistical analyses using Kruskal-Wallis ANOVA test, the *p*-value was lower than 0.05.

## DISCUSSION

Growing evidence indicate that synaptic dysfunction is a key process in the development of many neurodegenerative disorders including sCJD. Synaptic failure and loss can occur even before the onset of the clinical symptoms. For instance, scrapie-infected mice showed changes in motivational behavior long



time before the appearance of motor signs, and they correlated with the initial loss of presynaptic terminals in the dorsal hippocampus [15, 16]. In the Tg(PG14) mouse model of inherited prion disorders, expression of mutant PrP with 14 octapeptide repeats was associated with extended cell loss occurring in the cerebellum. Crossing these mice with Bax deficient mice rescued neuronal apoptosis. However, it rescued neither synaptic loss nor clinical symptoms suggesting that synaptic dysfunction rather than cell death makes a critical contribution to the Tg(PG14) mouse phenotype [17]. Moreover, reversing synaptic dysfunction can rescue neurons and prevent neuronal death at an early stage of the prion infection [18].

Involvement of different molecular partners and/or pathways might underlie the unusual degree of the clinical and pathological heterogeneity observed in sCJD. Indeed, our proteomic findings indicate that diverse molecular pathways could be involved in the pathogenesis of the MM1 and VV2 subtypes. Moreover, these data are in line with previous work on gene expression profiles in various subtypes of sCJD, where genes explicitly associated with MM1 subtype were reported [19].

Among 23 proteins with altered expression level in sCJD-affected brain, only one isoform of GFAP and spectrin alpha chain showed significant common differential expression in both analyzed sCJD subtypes. However, few further proteins displayed tendency to up- or down-regulation, though significance level was not reached in one of the analyzed subtypes. Western blot analysis of annexin A6, syntaxin-binding protein 1, and spectrin showed significant decrease in expression level in both subtypes, although significant regulation was reached in only one of sCJD subtypes in 2D gel analysis.

Thus, it is likely that other proteins showing changes in abundance without fulfilling statistical requirements to be classified as differentially expressed ( $p$ -value  $>0.05$ ) might reach significance in other experimental conditions.

Fig. 4. Western blot analysis of annexin A6 (A), syntaxin-binding protein 1 (B), and spectrin (C). All analyzed proteins showed significant down-regulation in both sCJD subtypes as compared to CON ( $p$ -value  $<0.05$  in Kruskal-Wallis ANOVA with Tukey's range test, indicated as \*). The representative blots are shown below graphs.  $\beta$ -actin expression was used as a control for an equal protein load. Expression level of each protein displayed by Western blot was quantified by densitometric analysis and presented as a graph. Data were normalized against  $\beta$ -actin and are given as a ratio of each protein/ $\beta$ -actin  $\pm$  SD and expression levels were analyzed in at least three patients per group.

The inclination to the more prominent proteome alterations was observed in the MM1 subtype. Interestingly, this phenomenon was not observed when soluble fractions of these brain homogenates (supernatants) were analyzed. However, the degree of subtype-specific proteome changes was maintained and comparable to those observed in synaptic fractions [20]. This might indicate that pathological changes at the synaptic level might be responsible for the heterogenic clinical picture of sCJD.

The accumulation of PrP aggregates is associated with various cellular morphological changes. In human embryonal teratocarcinoma NTERA2 cells (NT2) terminally differentiated into neuronal and glial cells, it was shown that rPrP fibrils could cause degeneration of neuronal processes. This degeneration was accompanied by the collapse of microtubules, aggregation of cytoskeletal proteins, and formation of neuritic beads [21]. The presence of PrP<sup>Sc</sup>, or even conversion of PrP<sup>C</sup> into PrP<sup>Sc</sup> itself, might disturb some specific protein-protein interactions with transporters or receptors leading to disruption of cell structure, impair communication between neurons, and finally to the cell death. Spectrin binds in a calcium-dependent manner to NMDA receptor, which in turn plays a critical role in synaptic activity, plasticity, and memory process [22, 23]. In addition, PrP<sup>C</sup> is involved in cell proliferation and in the distribution of junction-associated proteins, such as spectrin [24], which could suggest direct or indirect interaction between PrP<sup>C</sup> and spectrin. Thus, it is conceivable that PrP misfolding may lead to spectrin distribution failure and further to the synaptic dysfunction in neurons.

In the group of sCJD-associated proteins related to cell structure and transport, annexin A6, calcium, and phospholipid-binding protein requires special attention. Members of annexins A family are repeatedly mentioned in the context of the PrP biology [13, 19, 25, 26], therefore they may play some decisive role in the PrP pathophysiology.

Syntaxin-binding protein 1 (Munc18) plays an essential role in neurosecretion [27, 28] and its complex with X11 and syntaxin 1 prevents the interaction of amyloid- $\beta$  protein precursor (A $\beta$ PP) with BACE 1, thus inhibiting the amyloidogenic A $\beta$ PP  $\beta$ -cleavage. Furthermore, phosphorylation of syntaxin-binding protein 1 by the cyclin-dependent kinase 5 (Cdk5) induces A $\beta$ PP shift to the BACE 1-reach domain promoting  $\beta$ -cleavage of A $\beta$ PP [29]. Taken together, these findings might support a hypothesis on a molecular cross-talk between pathology of AD and prion diseases involving Cdk5 [30, 31]. Indeed, it was

shown that both PrP<sub>106-126</sub> and amyloid- $\beta$ <sub>1-40</sub> peptides can trigger Cdk5-mediated apoptotic neuronal death [32].

The overall picture deduced from our data indicates that over the course of sCJD, synaptic mitochondrial malfunction could occur, which negatively influences cell metabolism. This hypothesis is in line with finding showing that in neurodegenerative disorders aggregated proteins such as A $\beta$  or tau protein can induce oxidative stress leading to mitochondrial malfunction and finally to cell death [33]. Moreover, mitochondria play a crucial role in intracellular Ca<sup>2+</sup>-buffering at the synaptic compartment. Thus, their malfunction could result in disrupted calcium homeostasis. Indeed, prion-induced calcium dyshomeostasis and mitochondrial malfunction was already shown in cell culture models [34, 35]. In our study, at least five out of the 23 differentially expressed proteins are either calcium-binding or calcium-dependent, suggesting that calcium metabolism is an important factor in prion-induced neurodegeneration.

Moreover, our findings support a hypothesis of molecular cross-talk between pathological processes occurring in AD and prion disease. At least six of the differentially expressed proteins have been already associated with A $\beta$  pathobiology and AD. For example, alpha-crystallin, a small heat shock protein, is potent inhibitor of A $\beta$ <sub>1-40</sub> fibril formation in PC12 cell culture [36] but it also induces fragmentation of PrP fibrils *in vitro* [37].

The proteomic technologies give a unique opportunity to analyze biological processes at the protein level on the global scale. Knowledge about changes in the protein abundances and their modifications, as a consequence of a certain disease or induced by toxic agent, can bring new insight into pathological processes and can improve our understanding of underlying mechanisms. However, analysis of human brain tissue is limited to the analysis of the end-stage of the disease, where neurodegenerative changes are in the most advanced stage. The employment of an animal model allows investigation of the potential involvement of differentially expressed proteins found in human studies in the early stages of the disease or even in the pre-symptomatic phase. In our case, research on synaptic failure in sCJD could be approached by using mice expressing human PrP<sup>C</sup> or by a cellular model of primary cortical neurons both infected with brain homogenate from either the MM1 or VV2 subtype [38, 39]. This approach may help to understand the cascade of molecular events and to identify crucial steps for therapeutic intervention or early effective diagnostics.

## CONCLUSIONS

Taken together, differential regulation of proteins that we identified in this study could lead to significant disruption of synaptic activity and further to neuronal death. Special attention should be paid to the observation that several of these proteins have already been associated with mitochondrial function and calcium metabolism suggesting a probable role of mitochondrial malfunction and calcium homeostasis in prion-induced pathology.

Striking differences in altered proteome patterns between MM1 and VV2 subtypes may further support hypothesis that diverse molecular pathways and/or molecular partners are triggered by the different forms of misfolded PrP. And this, in turn, may result in the observed heterogeneous clinical and pathological sCJD phenotype.

Another interesting aspect is that many differentially expressed proteins found in this study were already associated with AD, suggesting the presence of molecular-cross talk between these neurodegenerative disorders or the implication of a common mechanism(s) underlying their pathophysiology, but further research is needed to solve this issue.

## ACKNOWLEDGMENTS

The study could be performed thanks to the German National Reference Center for TSE Surveillance.

The authors thank Barbara Ciesielczyk, Tatjana Pfander, Christa Scholz, and Christina Wiese for their outstanding technical help and valuable advices.

The study was supported by grant from European Commission PRIORITY KBBE-2007-2-4-06 "Protecting the food chain from prions: shaping European priorities through basic and applied research" and within the framework of the EU Joint Programme Neurodegenerative Disease Research - JPND - DEMTEST (01ED1201A).

Authors' disclosures available online (<http://www.j-alz.com/disclosures/view.php?id=1774>).

## SUPPLEMENTARY MATERIAL

A supplementary table containing MS data including MS/MS spectra for proteins identified from 3 or less peptides is visible in the electronic version of this article: <http://dx.doi.org/10.3233/JAD-130455>

## REFERENCES

- [1] Parchi P, Giese A, Capellari S, Brown P, Schulz-Schaeffer W, Windl O, Zerr I, Budka H, Kopp N, Piccardo P, Poser S, Rojiani A, Streichemberger N, Julien J, Vital C, Ghetti B, Gambetti P, Kretzschmar HA (1999) Classification of sporadic Creutzfeldt-Jakob disease based on molecular and phenotypic analysis of 300 subjects. *Ann Neurol* **46**, 224-233.
- [2] Gambetti P, Kong Q, Zou W, Parchi P, Chen SG (2003) Sporadic and familial CJD: Classification and characterisation. *Br Med Bull* **66**, 213-239.
- [3] Clinton J, Forsyth C, Royston MC, Roberts GW (1993) Synaptic degeneration is the primary neuropathological feature in prion disease: A preliminary study. *Neuroreport* **4**, 65-68.
- [4] Ferrer I, Puib B, Blanco R, Martí E (2000) Prion protein deposition and abnormal synaptic protein expression in the cerebellum in Creutzfeldt-Jakob disease. *Neuroscience* **97**, 715-726.
- [5] Jeffrey M, Halliday WG, Bell J, Johnston AR, MacLeod NK, Ingham C, Sayers AR, Brown DA, Fraser JR (2000) Synapse loss associated with abnormal PrP precedes neuronal degeneration in the scrapie-infected murine hippocampus. *Neuropathol Appl Neurobiol* **26**, 41-54.
- [6] Sisková Z, Sanyal NK, Orban A, O'Connor V, Perry VH (2010) Reactive hypertrophy of synaptic varicosities within the hippocampus of prion-infected mice. *Biochem Soc Trans* **38**, 471-475.
- [7] Bouzamondo-Bernstein E, Hopkins SD, Spilman P, Uyehara-Lock J, Deering C, Safar J, Prusiner SB, Ralston HJ 3rd, DeArmond S (2004) The neurodegeneration sequence in prion diseases: Evidence from functional, morphological and ultrastructural studies of the GABAergic system. *J Neuropathol Exp Neurol* **63**, 882-899.
- [8] Brown P, Rohwer RG, Gajdusek DC (1986) Newer data on the inactivation of scrapie virus or Creutzfeldt-Jakob disease virus in brain tissue. *J Infect Dis* **153**, 1145-1148.
- [9] Tateishi J, Tashima T, Kitamoto T (1991) Practical methods for chemical inactivation of Creutzfeldt-Jakob disease pathogen. *Microbiol Immunol* **35**, 163-166.
- [10] Prusiner SB, Groth D, Serban A, Stahl N, Gabizon R (1993) Attempts to restore scrapie prion infectivity after exposure to protein denaturants. *Proc Natl Acad Sci U S A* **90**, 2793-2797.
- [11] Yao HL, Han J, Gao JM, Zhang J, Zhang BY, Guo YJ, Nie K, Gao C, Wang XF, Dong XP (2005) Comparative study of the effects of several chemical and physical treatments on the activity of protease resistance and infectivity of scrapie strain 263K. *J Vet Med B Infect Dis Vet Public Health* **52**, 437-443.
- [12] Candiano G, Bruschi M, Musante L, Santucci L, Ghiggeri GM, Carnemolla B, Orecchia P, Zardi L, Righetti PG (2004) Blue silver: A very sensitive colloidal Coomassie G-250 staining for proteome analysis. *Electrophoresis* **25**, 1327-1333.
- [13] Ramljak S, Asif AR, Armstrong VW, Wrede A, Groschup MH, Buschmann A, Schulz-Schaeffer W, Bodemer W, Zerr I (2008) Physiological role of the cellular prion protein (PrP<sub>c</sub>): Protein profiling study in two cell culture systems. *J Proteome Res* **7**, 2681-2695.
- [14] Asif AR, Oellerich M, Armstrong VW, Gross U, Reichard U (2010) Analysis of the cellular *Aspergillus fumigatus* proteome that reacts with sera from rabbits developing an acquired immunity after experimental aspergillosis. *Electrophoresis* **31**, 1947-1958.

- [15] Guenther K, Deacon R, Perry VH, Rawlins JN (2001) Early behavioural changes in scrapie-affected mice and the influence of dapsone. *Eur J Neurosci* **14**, 401-409.
- [16] Cunningham C, Deacon R, Wells H, Boche D, Waters S, Diniz CP, Scott H, Rawlins JN, Perry VH (2003) Synaptic changes characterize early behavioural signs in the ME7 model of murine prion disease. *Eur J Neurosci* **17**, 2147-2155.
- [17] Chiesa R, Picardo P, Dossena S, Nowoslowski L, Roth KA, Ghetti B, Harris DA (2005) Bax deletion prevents neuronal loss but not neurological symptoms in a transgenic model of inherited prion disease. *Proc Natl Acad Sci U S A* **102**, 238-243.
- [18] Moreno JA, Mallucci GR (2010) Dysfunction and recovery of synapses in prion disease: Implications for neurodegeneration. *Biochem Soc Trans* **38**, 482-487.
- [19] Xiang W, Windl O, Westner IM, Neumann M, Zerr I, Lederer RM, Kretschmar HA (2005) Cerebral gene expression profiles in sporadic Creutzfeldt-Jakob disease. *Ann Neurol* **58**, 242-257.
- [20] Gawinecka J, Cardone F, Asif AR, De Pascalis A, Wemheuer WM, Schulz-Schaeffer WJ, Pocchiari M, Zerr I (2012) Sporadic Creutzfeldt-Jakob disease subtype-specific alterations of the brain proteome: Impact on Rab3a recycling. *Proteomics* **12**, 3610-3620.
- [21] Novitskaya V, Makarava N, Sylvester I, Bronstein IB, Baskakov IV (2007) Amyloid fibrils of mammalian prion protein induce axonal degeneration in NTERA2-derived terminally differentiated neurons. *J Neurochem* **102**, 398-407.
- [22] Wechsler A, Teichberg VI (1998) Brain spectrin binding to the NMDA receptor is regulated by phosphorylation, calcium and calmodulin. *EMBO J* **17**, 3931-3939.
- [23] Morgado-Bernal I (2011) Learning and memory consolidation: Linking molecular and behavioral data. *Neuroscience* **176**, 12-19.
- [24] Morel E, Fouquet S, Strup-Perrot C, Pichol Thievent C, Petit C, Loew D, Faussat AM, Yvernault L, Pinçon-Raymond M, Chambaz J, Rousset M, Thenet S, Clair C (2008) The cellular prion protein PrP(c) is involved in the proliferation of epithelial cells and in the distribution of junction-associated proteins. *PLoS One* **3**, e3000.
- [25] Weiss E, Ramljak S, Asif AR, Ciesielczyk B, Schmitz M, Gawinecka J, Schulz-Schaeffer W, Behrens C, Zerr I (2010) Cellular prion protein overexpression disturbs cellular homeostasis in SH-SY5Y neuroblastoma cells but does not alter p53 expression: A proteomic study. *Neuroscience* **169**, 1640-1650.
- [26] Zafar S, von Ahsen N, Oellerich M, Zerr I, Schulz-Schaeffer WJ, Armstrong VW, Asif AR (2011) Proteomics approach to identify the interacting partners of cellular prion protein and characterization of Rab7a interaction in neuronal cells. *J Proteome Res* **10**, 3123-3135.
- [27] Han GA, Malintan NT, Collins BM, Meunier FA, Sugita S (2010) Munc18-1 as a key regulator of neurosecretion. *J Neurochem* **115**, 1-10.
- [28] Hata Y, Slaughter CA, Südhof TC (1993) Synaptic vesicle fusion complex contains unc-18 homologue bound to syntaxin. *Nature* **366**, 347-351.
- [29] Sakurai T, Kaneko K, Okuno M, Wada K, Kashiyama T, Shimizu H, Akagi T, Hashikawa T, Nukina N (2008) Membrane microdomain switching: A regulatory mechanism of amyloid precursor protein processing. *J Cell Biol* **183**, 339-352.
- [30] Baier M, Apelt J, Riemer C, Gültner S, Schwarz A, Bamme T, Burwinkel M, Schliebs R (2008) Prion infection of mice transgenic for human APPSwe: Increased accumulation of cortical formic acid extractable Abeta(1-42) and rapid scrapie disease development. *Int J Dev Neurosci* **26**, 821-824.
- [31] Morales R, Estrada LD, Diaz-Espinoza R, Morales-Scheihing D, Jara MC, Castilla J, Soto C (2010) Molecular cross talk between misfolded proteins in animal models of Alzheimer's and prion diseases. *J Neurosci* **30**, 4528-4535.
- [32] Lopes JP, Oliveira CR, Agostinho P (2007) Role of cyclin-dependent kinase 5 in the neurodegenerative process triggered by amyloid-Beta and prion peptides: Implications for Alzheimer's disease and prion-related encephalopathies. *Cell Mol Neurobiol* **27**, 943-957.
- [33] Grimm S, Hoehn A, Davies KJ, Grune T (2011) Protein oxidative modifications in the ageing brain: Consequence for the onset of neurodegenerative disease. *Free Radic Res* **45**, 73-88.
- [34] O'Donovan CN, Tobin D, Cotter TG (2001) Prion protein fragment PrP-(106-126) induces apoptosis via mitochondrial disruption in human neuronal SH-SY5Y cells. *J Biol Chem* **276**, 43516-43523.
- [35] Ferreira E, Oliveria CR, Pereira CM (2008) The release of calcium from the endoplasmic reticulum induced by amyloid-beta and prion peptides activates the mitochondrial apoptotic pathway. *Neurobiol Dis* **30**, 331-342.
- [36] Dehle FC, Ecroyd H, Musgrave IF, Carver JA (2010)  $\alpha$ B-Crystallin inhibits the cell toxicity associated with amyloid fibril formation by  $\kappa$ -casein and the amyloid- $\beta$  peptide. *Cell Stress Chaperones* **15**, 1013-1026.
- [37] Sun Y, Makarava N, Lee CI, Laksanalamai P, Robb FT, Baskakov IV (2008) Conformational stability of PrP amyloid fibrils controls their smallest possible fragment size. *J Mol Biol* **376**, 1155-1167.
- [38] Carimalo J, Cronier S, Petit G, Peyrin JM, Boukhtouche F, Arbez N, Lemaigre-Dubreuil Y, Brugg B, Miquel MC (2005) Activation of the JNK-c-Jun pathway during the early phase of neuronal apoptosis induced by PrP106-126 and prion infection. *Eur J Neurosci* **21**, 2311-2319.
- [39] Cronier S, Beringue V, Bellon A, Peyrin JM, Laude H (2007) Prion strain- and species-dependent effects of antiprion molecules in primary neuronal cultures. *J Virol* **81**, 13794-13800.